Why Bitcoin and Ethereum Differ in Transaction Costs:

A Theory of Blockchain Fee Policies

Abdoulaye Ndiaye[*]

New York University

February 26, 2024

First Version: July 27, 2023

Abstract

Blockchains, the technology underlying cryptocurrencies, face large fluctuations in user demand and marginal costs. These fluctuations make effective fee policies necessary to manage transaction service allocation. This paper models the conflict between the blockchain designer and validators with monopoly power in choosing between price-setting and quantity-setting fee policies. The key determinants of the advantage of price-setting on blockchains are the validators' bargaining power, the elasticity of demand, the validators' uncertainty about demand, and the covariance of demand and marginal costs. My results help account for differences between the fee policy designs of Bitcoin and Ethereum, the leading blockchains, and have implications for how they can be improved.

Keywords: Blockchain, Transaction Costs, Fee Policies, Bitcoin, Ethereum, Demand Fluctuations, Price Elasticity

1 Introduction

Over the last fifteen years, cryptocurrencies have experienced remarkable growth, with their combined market capitalization reaching a peak of $3 trillion in 2021. The technology at the heart of cryptocurrencies—blockchain—has emerged as a potent tool for facilitating efficient peer-to-peer transactions. However, the volatile nature of the market has led to significant fluctuations in transaction demand and in marginal costs for blockchain technology services. In response to this uncertainty, blockchain designers are increasingly employing fee policies or transaction fee mechanisms (TFMs) to allocate the finite block space effectively.

The Bitcoin and Ethereum blockchains are two leading examples that reflect opposite extremes in the choice of fee policies. For Bitcoin fees, a maximum quantity is set by the protocol (maximum block size), and fees are independently chosen by users and transaction service providers. I call this the quantity-setting or quantity controls regime. Ethereum, on the other hand, sets a minimum price, while the block size adjusts in response to demand. I call this the price-setting or price controls regime. Most blockchains follow a variation of either the Bitcoin or the Ethereum fee policies, and some set constant fees by default or subsidize user fees until their network matures and faces congestion issues. In addition, there is an active debate on the future of the Bitcoin blockchain: as the payoff for transaction service providers programmatically decreases every four years, the role of fees becomes increasingly important for Bitcoin.

In this paper, I model a blockchain—similar to that underlying Bitcoin or Ethereum—as a distributed computing network where users submit transactions for inclusion by validators—the transaction service providers. Transactions, representing data that modify the network's state (such as account balance transfers), are submitted by users with a bid to a publicly observable pool—known as the mempool—that indicates their willingness to pay for their transactions to be processed. Validators, using their limited resources, select a subset of transactions from the mempool to form a block. Each block, comprising an ordered sequence of transactions and a reference to the previous block,

can be appended to the blockchain in every period. However, technological limitations impose a maximum block size, thereby constraining the supply of block space.

On the supply side, validators face fluctuations in their marginal costs. In a proof-of-work protocol such as Bitcoin, validators (called miners) use computational resources to solve a mathematical puzzle, and their marginal cost varies with the level of competition that they face before being selected to validate transactions. In a proof-of-stake protocol such as the updated Ethereum, marginal costs are essentially constant.

On the demand side, atomistic users arrive at random and submit their transactions along with their willingness to pay for these transactions to be included in the next block. Given the paper's focus on the aggregate properties of the block space market, I operate under the assumption that users bid their true valuations.[1] This process forms the microfoundations of an aggregate user demand curve, with a demand shifter that captures situations of low and high demand.

In the face of these uncertainties, the protocol needs to commit to either a base fee—an ex ante price control—or a block size limit—an ex ante quantity control. This choice highlights a disagreement between the blockchain designers' objective and the profit-maximization objective of validators with significant monopoly power after they are chosen to validate a block. Indeed, a protocol designer who prefers full capacity utilization or has an exogenous technological block size target (that internalizes social benefits and costs) will prefer the quantity-setting regime as it guarantees the preferred block size irrespective of sources of uncertainty. A monopolist validator, on the other hand, would prefer either the price-setting or the quantity-setting regimes, depending on the relative degree of uncertainty in demand and marginal costs.

I model the resolution of the conflict between the blockchain designer's and monopolistic validator's preferences through Nash bargaining over the protocol profits. I show that, in this context, the choice of instruments is more nuanced than Weitzman's (1974) "prices vs. quantities" insight: namely, that price controls prove more effective

---

[1]Dominant-strategy incentive compatibility for all the TFMs considered in this paper is substantiated by the game-theoretic proofs provided by Roughgarden (2020, 2021).

when demand uncertainty is high and quantity controls more effective when uncertainty in marginal costs is high. In general, the key determinants of the advantage of price-setting in blockchains are the validators' bargaining power, the elasticity of demand, the validators' uncertainty about demand, and the covariance of demand and marginal costs.

First, when validators have high bargaining power, demand uncertainty favors price controls, as block size adjustments provide the flexibility necessary to accommodate demand fluctuations. Second, a positive correlation between marginal costs and demand disfavors price controls. In this case, quantity adjustments would lead to the production of larger blocks when marginal costs are high, thereby decreasing efficiency. Third, a higher price elasticity of demand—the proportional change in block space demand in response to a proportional change in price for the marginal user seeking to include her transaction in the next block—further amplifies the relative advantage of price controls over quantity controls and makes the choice over fee policies even more important. However, if the monopolist validator has low bargaining power, quantity controls become more effective. Last, in the absence of uncertainty, the blockchain designer and validator remain indifferent between price and quantity controls.

This result helps us understand the differences in the policies that determine fees and block space in Bitcoin and Ethereum. For both blockchains, price elasticity of demand is high, and demand uncertainty is significant.

Ethereum can be viewed through the lens of our model as an instance where the validators have high bargaining power (or are considered influential by the protocol designers). In addition, since its proof-of-stake upgrade, the marginal cost of a marginal block increase for Ethereum validators is virtually constant. In this case, my result points to price-setting as the most favorable policy for Ethereum. This helps explain the recent adoption of the Ethereum Improvement Proposal 1559's (EIP-1559's) price-setting policy for the Ethereum blockchain. Furthermore, Ethereum's fee policies are found to perform better after Ethereum's proof-of-stake upgrade, consistent with the correlation between validators' marginal costs and demand relative to miners' being

4

lower in a proof-of-work protocol.

Bitcoin, for its part, is distinguished as the first blockchain with an anonymous founder, and its core developers strongly emphasize decentralization and censorship resistance. Most proposals to change Bitcoin's fees and block size policies have failed. Bitcoin can therefore be viewed through the lens of my model as an instance where validators (here miners) have low bargaining power (or are not attributed enough importance by protocol designers). In addition, under the proof-of-work protocol, the marginal cost of miners is largely positively correlated with demand. Our result then states that, in this case, price-setting is less effective than in the case of Ethereum.

Last, it is important to consider that users (and validators) might value block space (and marginal costs) in dollars or in real terms rather than in the native currency of the blockchain. To accommodate this, I expand the model to introduce uncertainty in the price of the cryptocurrency in US dollars or in real terms. Notably, price controls are restricted to be expressed in units of the native currency. I show that volatility in the cryptocurrency price reduces the advantage of price controls over quantity controls.

Building on these insights, I briefly discuss the implications of my results for fee policies on Ethereum, the most widely utilized public blockchain, whose fee policy is a blueprint for many blockchains that follow the price-setting regime. I show that the rate at which Ethereum's fee policies readjust prices should be tightly linked to the price elasticity of demand for inclusion of a transaction in the next block. I apply my framework to evaluate recent changes to Ethereum's fee policies using a random sample of Ethereum transaction data. I find that the rate at which Ethereum's fees are changed is faster than optimal.

In addition, I investigate the optimal block size target (a quantity control) for a monopolistic validator and offer tight bounds on its size relative to the block size limit. There are widespread concerns regarding the potential for validators and other users to exploit their power to capture what is colloquially referred to as *"maximal extractable value"* (MEV) through the censoring, swapping, and front-running of mempool transactions (Daian et al., 2020). I find that Ethereum's current ratio of block size target to

maximum block size leaves too much room for monopolist validators to include their own value-extracting transactions.

Blockchain designers need simple and robust economic insights for designing their fee policies. With this need in mind, I conclude by suggesting open questions that are connected to this research.

1.1 Literature Review

The literature has generally explained blockchain fees as arising because of competition for block space among heterogeneous, impatient users (Huberman et al., 2021). Easley et al. (2019) study the evolution of Bitcoin transaction fees, while Hinzen et al. (2022) highlight Bitcoin's limited adoption problem. Some studies highlight the strategic use of capacity on the Bitcoin blockchain (Lehar and Parlour, 2020; Malik et al., 2022). Catalini and Gans (2020) provide a simple primer on the economics of blockchains.

This paper contributes to the literature on price versus quantity controls, a domain pioneered by Weitzman (1974). The issue of choosing a supply function under uncertainty has been explored in Klemperer and Meyer (1989). My approach aligns closely with that of Reis (2006) and Flynn et al. (2023), who scrutinize the choice of a supply function from a firm's perspective and its macroeconomic implications. While my work draws inspiration from Weitzman (1974), it diverges in that it contemplates the planner's (blockchain designer's) problem with a variety of goals, including purely technical objectives like those seen in practice, such as block size targets. The conclusions of this analysis are then applied to the design of TFMs. Specifically, Ndiaye (2024) provides a summary of how the economic factors that affecting the design of TFMs, as studied in this paper, correlate with the technical features of blockchains.

The literature taking a microeconomic mechanism design perspective to examine fee policies (TFMs) is growing. Notably, Akbarpour and Li (2020) examine mechanisms immune to designer manipulations—referred to as "credible mechanisms"—and demonstrate that the well-known second-price auction does not meet this credibility criterion. In the blockchain context, Roughgarden (2021) applies this credibility condi-

tion to TFMs and establishes that EIP-1559, Ethereum's TFM, which essentially acts as a first-price auction with a dynamic reserve price, and its variations are incentive-compatible for users and adhere to a form of myopic credibility for validators. These findings are further consolidated by Chung and Shi (2023). These papers provide game-theoretic foundations that guarantee that the ADT-TFMs (transaction fee mechanisms that are adaptive to a deterministic target) that I study are incentive compatible. Ferreira et al. (2021) explore an alternative aspect of TFMs by investigating posted price mechanisms. The approach that I take in is paper is complementary to this strand of literature. Moreover, I delve into the dynamics of TFMs, offering insights into their updating rules.

This paper also advances the literature examining the block space market from a macroeconomic perspective. The concepts formalized in Section 3 of this paper build upon and extend Buterin's (2018) reading of Weitzman (1974), with important differences characterizing the blockchain context due to the fact that the protocol designer is limited in her capacity to enforce quantity or price controls. In other related work, Lavi et al. (2022) and Nisan (2023) investigate the monopolistic market for unlimited block space, in contrast to this paper, which takes the block size limit as an exogenous technological constraint.

Last, this paper contributes to studies of the dynamics of the Ethereum fee policies recently adopted in EIP-1559. Leonardos et al. (2021) delve into the behavior of the dynamic system resulting from the TFM, and Leonardos et al. (2022) uncover numerous empirical properties for which this paper provides a theoretical explanation.

Outline: The paper is organized as follows: Section 2 gives an overview of the functioning of the Bitcoin and Ethereum protocols, makes the case that validators have had more bargaining power in the history of Ethereum than in that of Bitcoin, and explains how Ethereum fees are determined. Section 3 introduces the model and provides the main results of my analysis and an extension to cryptocurrency price fluctuations. Section 4 examines implications for Ethereum's fee policies. Last, Section 5 concludes the

paper.

2 Fees and Block Space Utilization in Bitcoin and Ethereum Protocols

2.1 Bitcoin and Ethereum Protocols

A blockchain is a decentralized digital ledger that records transactions across a network of computers, called validators, in an immutable chained list of blocks. Bitcoin, introduced by Nakamoto (2008), was conceived as a peer-to-peer digital currency. In contrast, Ethereum, proposed by Buterin et al. (2013), extends the basic blockchain concept to include more versatile functionalities such as self-executing agreements, known as "smart contracts".

In both Bitcoin and Ethereum, each block has a fixed capacity because of technological constraints such as bandwidth and storage and the negative externalities associated with large blocks' propagation times. These limitations are designed to ensure that running a node remains accessible to a broad range of participants, thereby fostering decentralization. This limited capacity necessitates the use of transaction fees, which serve as a market mechanism to allocate this scarce resource. Fees incentivize validators to prioritize and include transactions in a block.

Over the years, both Bitcoin and Ethereum have experienced changes in their block capacity and fee structures to adapt to changing network demands. On the price side, Bitcoin shifted from offering no-fee transactions to imposing transaction fees, as studied by Easley et al. (2019). On the block capacity side, since its inception, Bitcoin has given control of this capacity to the protocol developers. The original 1MB block size limit in the Bitcoin blockchain ignited intense debates within the community over scalability versus decentralization. On one side, proponents of a larger block size argued that increasing capacity would enable more transactions per block, alleviating congestion and lowering fees. On the other side, critics warned that larger blocks would raise the

computational and storage requirements for running a validator, thereby compromising the network's decentralization. This ideological divide reached its peak in 2017, leading to a "hard fork" that birthed Bitcoin Cash, a separate chain with an 8MB block size. Concurrently, Bitcoin adopted Segregated Witness (SegWit), effectively changing the block size limit to a more complex "block weight" limit of approximately 4 million units.

Ethereum, for its part, imposed transaction fees from the beginning. In Ethereum, "gas" serves as the unit of resources, and the "gas limit" dictates the maximum network capacity in a single block. Initially, Ethereum attempted a different paradigm and gave control over capacity to validators. Each validator was allowed to change capacity up or down by 0.1% for each new block. The underlying rationale was to transform the philosophical debate on block size into an economic decision, with the assumption that validators, heavily invested in the network, would act individually in the long-term interest of the network. However, in practice, the history of Ethereum block size changes in Table A1 in Appendix A illustrates that validators have often abused their bargaining power and colluded to manipulate network capacity. This behavior is exemplified by an April 21, 2021, announcement from Sparkpool, a major Chinese validator with 23.5% of the network's computational power at that time:

```
@sparkpool_eth:  "We are raising gas limit to 15 million"
@btcdentist:  "did you get permission from the core devs?"
@sparkpool_eth:  "What we need is advice from dev, not permission."
```

To curb such practices, Ethereum introduced EIP-1559, a fee mechanism designed to both limit validators' discretionary power over network capacity and enhance fee predictability for users.

Figure 1 illustrates the time series of the capacity utilization rates of the Bitcoin and Ethereum blockchains. Taking into account the upgrades within blockchains over time and variations across blockchains, I define the block size target as the size below which the reserve price for pending transactions does not increase. The capacity utilization rate is, consequently, the daily average of the fraction of the realized block size to the block size target.
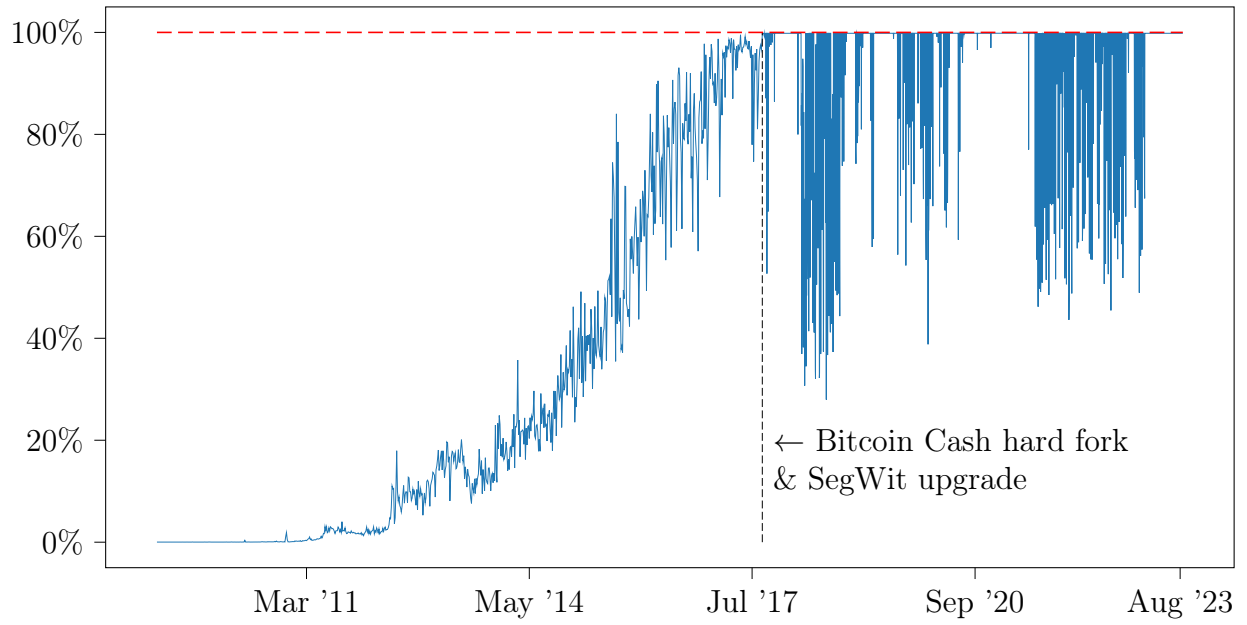
(a) Bitcoin capacity utilization rate per day
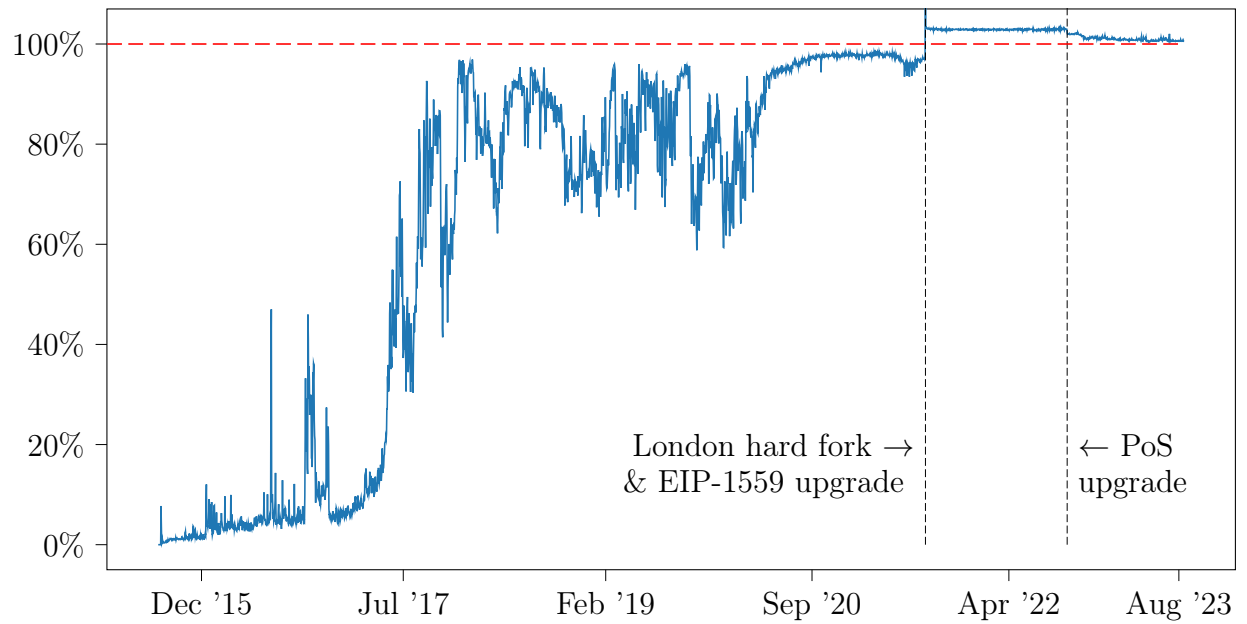
(b) Ethereum capacity utilization rate per day

Figure 1: Time series of Bitcoin and Ethereum capacity utilization rates

For Bitcoin, the block size target was 1MB pre-SegWit and is 4 million weights post-upgrade. The top panel indicates an initial surge in Bitcoin's utilization rate during its nascent phase. However, as its use has become more widespread, the network has not always operated at full capacity. This is corroborated by Lehar and Parlour (2020), who attribute the prevalence of less-than-full blocks to strategic capacity management by monopolistic validators.

Prior to the London hard fork, Ethereum's block size target varied based on validator votes, ranging from 3.1 million to 15 million gas, as detailed in Appendix A. Post–London fork and EIP-1559 implementation, the target is a fixed 15 million gas, with an upper limit of 30 million and a dynamic reserve price adjustment for pending transactions to align closely with the target. The bottom panel reveals that, just as for Bitcoin, Ethereum's early-phase utilization rate rose steadily. However, following the introduction of EIP-1559 via the London hard fork, the blockchain has operated at full capacity. My analysis attributes this to EIP-1559's design, arguing that transaction fees now effectively shape and regulate the supply curve for monopolistic validators.

Such economic interactions between fee mechanisms and capacity have been overlooked in earlier studies. For instance, Lehar and Parlour (2020) focus on strategic capacity utilization in Bitcoin, while Huberman et al. (2021) theoretically ascribe full capacity utilization to the free entry of validators even though Bitcoin does not always operate at full capacity despite such entry. In my analysis in Appendix B.1, I examine factors affecting block space demand, including the number of active addresses, token prices, transaction fees, and residual demand through mempool size for Bitcoin. The data reveal strong correlations between traditional demand-side factors such as active addresses and transaction fees with the utilization rate for both Bitcoin and Ethereum pre-EIP-1559. Post-EIP-1559, these factors became decoupled from block utilization.

In my study on block space supply in Appendix B.2, I evaluate factors such as computing power and mining pool concentration for both Bitcoin and Ethereum, adding the total Ethereum staked and validator pool concentration for Ethereum post–proof of stake. The results indicate that neither computing power nor Ethereum staked signif-

icantly impact block utilization rates for either Bitcoin or Ethereum. However, higher concentration rates among mining pools in Bitcoin, measured through the Herfindahl–Hirschman index (HHI), correlate with sub-100% block utilization, suggesting that miners may exercise market power to leave blocks less full. This pattern does not hold for Ethereum, where both before and after the transition to proof of stake, mining pool concentration shows no discernible effect on block utilization rates. The stabilization of Ethereum's block utilization post–London fork further corroborates this observation.

2.2 Fees on Ethereum

Ethereum fees initially operated on a bidding system constrained by a fixed block size. The fixed per-block gas limit and fluctuations in demand resulted in delays for users, as the system lacked a "slack" mechanism to adjust block size to meet varying demand. In addition, since validators collected the fees, this system led to a first-price auction when demand was high. As first-price auctions are not incentive-compatible when user valuations are unobserved, this required complex fee estimation efforts from users.

With EIP-1559, Ethereum's fee structure underwent significant changes to address the issues with the first-price auction with a fixed block size limit. The system now operates with a target block size set at $q^{target} = 15M$ gas, a legacy from the pre–London hard fork settings, and a maximum block size of of $q^{\max} = 2q^{target}$. On the user end, each transaction comes with a "base fee", algorithmically adjusted based on network demand. The minimum gas price, p_t, is adjusted based on the formula

$$p_t = p_{t-1} \cdot (1 + d\frac{q_{t-1} - q^{target}}{q^{target}}) \tag{1}$$

where d is an adjustment parameter set to $\frac{1}{8}$, allowing the minimum price to double in 8 blocks when blocks are full. In addition to the base fee, users can include a "tip" to incentivize faster processing by validators. The dual-fee structure allows more predictability in transaction costs, as the base fee aligns closely with network congestion. Figure 2 shows fee settings and an estimator of the base fee for Ethereum users.

12

(a) User price choice from Meta-mask wallet
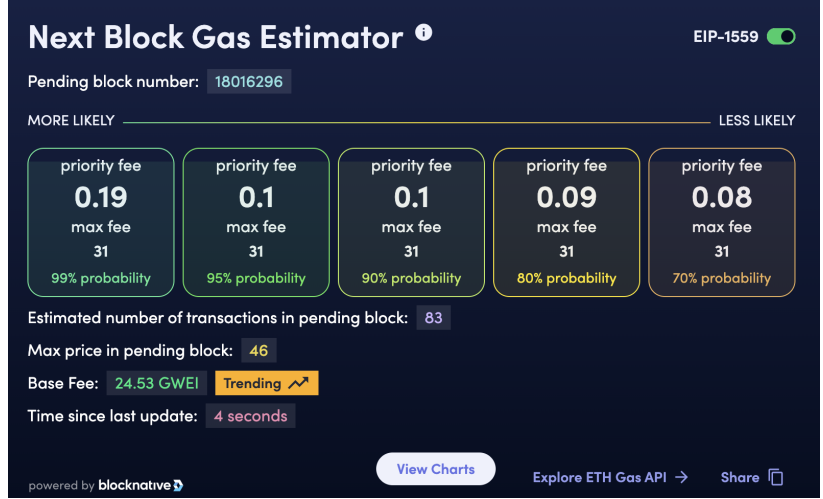
(b) Base fee and priority fee estimator from Blocknative

Figure 2: Ethereum fee settings and estimator

From a validator's standpoint, selection is stochastic, contingent on either the proof-of-work or proof-of-stake mechanism. Though validators enjoy a monopolistic position during their turn to validate a block, the protocol's fee structure regulates their behavior. Each transaction j carries a computational cost q_j, measured in gas units. Ethereum transaction senders pay an amount computed as $q_j \cdot \min\{p_t + \delta_j, c\}$, where δ_j is the tip and c the fee cap, with $c \geq p_t$. Incentive compatibility requires that, under normal demand conditions, the base fee adjusts upward to match the willingness to pay of the marginal user, and the tip is small in proportion. The aggregate base fee revenue, $\sum_{j=1}^{N} q_j p_t$, is "burned", primarily to address validators' off-chain incentives, as argued by Roughgarden (2021). Meanwhile, tips and a block reward go directly to the validator. By diverting a portion of the revenue away from the validator, the protocol has instruments to ensure that supply is not artificially restricted and that transactions of higher value are included.

EIP-1559 raises several questions regarding its rationale, potential for improvement, and the design of other fee policies that share its simplicity. Specifically, in the face of

demand fluctuations, why might a protocol designer opt for a blockchain with an imposed quantity limit as in Bitcoin and Ethereum pre–London hard fork and dynamically adjust when demand fluctuates vs. one where price controls such as the EIP-1559 base fee are imposed and dynamically adjust when demand fluctuates? What determines the shape and parameters of such transaction fees? These questions will be the focus of subsequent sections in this paper.

3 Model

3.1 Environment

A *blockchain*, such as Bitcoin or Ethereum, is modeled as a distributed computer network where users submit *transactions* to be included in a chain of *blocks* by *validators*. The blockchain maintains a record of the network's state, such as account balances. A transaction t represents arbitrary data sent over the network to alter its state—for instance, to transfer a balance. Users submit transactions to a publicly observed pool of outstanding transactions (*mempool*), with a bid b_t, signifying their willingness to pay for transaction processing. Monopolistic validators, using quantities x_i of a finite number of resources $i \in [\![1, N]\!]$ (e.g., computation, bandwidth), select a subset of transactions from the mempool to form a block. A block of size q is an ordered sequence of transactions and a reference to the previous block. Validators add a block to the blockchain by a consensus mechanism (such as proof of work or proof of stake), a process irrelevant to this analysis. Technological constraints impose a maximum block size $q^{\max}$, thus limiting the supply of block space.[2]

Validators: Validators use a bundle of computational resources $x \in \mathbb{R}_+^N$ priced at per-unit resource rates $p_x \in \mathbb{R}_{++}^N$ to produce a block of size $q \leq q^{\max}$, as given by

$$q = \sum_{i=1}^{N} p_{x_i} x_i \tag{2}$$

---

[2]See the related discussion in Buterin (2018) for the case of the Ethereum blockchain.

Validators incur a technological cost of $C(q) = c(x_1, \ldots, x_N)$ when producing a block. These costs encompass validation operation costs and other costs associated with accessing and modifying the blockchain's state. From the blockchain designer's viewpoint, costs might also include delays in block propagation due to the presence of large blocks and other societal costs. These costs, denoted by $C(q; \eta)$, are subject to uncertainty, represented by the distribution η.

Users: User transactions populate the mempool according to a stochastic process. I posit that users, denoted by $j \in [0, 1]$, are atomistic, with arrivals between two consecutive blocks, B_t, B_{t+1}, being independently and identically distributed according to a Poisson process X with a parameter of $\lambda q^{\max}$, where $\lambda \in \mathbb{R}_{++}$. For simplicity, I assume that users leave the pool if their transaction is not included in the next block, only to return according to the arrival process.[3]

Each user j has a valuation v_j drawn from a common distribution f with a cumulative distribution function F, which is continuous and increasing.

Establishing a Demand Curve: Given that the TFMs under consideration are dominant-strategy incentive-compatible, as demonstrated by Roughgarden (2021), it is reasonable to assume that users bid their true valuations, i.e., $b_t = v_j$. Consequently, for a given minimum bid for transaction inclusion, denoted by p, the number of users willing to pay the bid is $\lambda q^{\max} \bar{F}(p)$, where $\bar{F}(p) = 1 - F(p)$. The following lemma shows that this model serves as the microfoundation of an intuitive demand curve for block space, thereby linking demand parameters to model primitives.

Lemma 1. *The aggregate demand for block space can be represented as $p = \left(\bar{F} \right)^{-1} \left(\dfrac{q}{\Psi} \right)$, where the price elasticity of demand for the marginal user equals the tail ratio $\dfrac{p f(p)}{1 - F(p)}$.*

Specifically, when F is a Pareto distribution with scale p_m and shape α, the aggregate

---

[3]Leonardos et al. (2021) confirm that this assumption does not significantly impact the dynamics of transaction fees, which are the focus of our analysis. In his research, Nisan (2023) accounts for residual demand in the mempool and finds transaction fee dynamics similar to those in Leonardos et al. (2022).

demand for block space is given by

$$\frac{p}{p_m} = \left(\frac{q}{\Psi}\right)^{-\frac{1}{\varepsilon}} \tag{3}$$

Here, $p \in \mathbb{R}_+$ is the market price, $\Psi \equiv \lambda q^{\mathrm{max}}$ is a demand shifter, and $\varepsilon = \alpha$ is the price elasticity of demand for block space.

Proof. Refer to Appendix C.1 for the proof. □

In Section 3.3, I will assume that the user valuation distribution is Pareto unless otherwise stated. The assumption of a Pareto distribution is not restrictive. For a general user valuation distribution, one can calculate the price elasticity of demand at all points from the tail ratio of the distribution. Using data from the Ethereum blockchain, I fit a Pareto distribution to the transaction in Section **??**. This demand curve will prove useful when I consider uncertainty in the user arrival rate λ leading to uncertainty in the demand shifter Ψ. When $\lambda > 1$, we encounter a high-demand scenario where not all transactions can be included in the next block, whereas $\lambda < 1$ reflects a low-demand scenario where the block is not filled to capacity. Given this context and considering the uncertainties in both the cost $C(q; \eta)$ and demand Ψ, I explore the conditions under which a blockchain protocol designer would find it beneficial to introduce price or quantity controls.

3.2 Tension Between Protocol Objectives and Validators' Incentives

3.2.1 Protocol Designer's Preference for Maximum Capacity Utilization

If the protocol designer has a preference over the block size, then she will prefer quantity controls over price controls as the former insulates this variable from demand fluctuations. To illuminate the potential conflict between the protocol designer's objectives

and the miners' incentives, consider the following examples of objective $S(q)$ for the protocol designer.

Example 2. *(Social Welfare) Let u be an increasing function representing the utility of a representative user on the blockchain. The social welfare function $S(q)$ can be defined as*

$$S(q) = \begin{cases} u(q) & \text{if } q \leq q^{limit} \\ -\infty & \text{if } q > q^{limit} \end{cases} \tag{4}$$

This reflects the protocol designer's concern for maximizing user utility, an objective that can diverge from the profit-maximizing motives of validators.

Claim 3. *If 0 is in the support of Ψ, then the protocol designer would prefer to have blocks at full capacity. The only price that aligns with the designer's objective is zero.*

Proof. If the protocol designer can choose the block size, then she can guarantee a maximal utility at q^{limit}. With a price choice, however, we have $q = \max\{\Psi \left(\frac{p_m}{p}\right)^\varepsilon, q^{limit}\}$. This means that for any price p, there is a loss when demand intensity is low, $\Psi \leq \left(\frac{p}{p_m}\right)^\varepsilon q^{limit}$, which makes the expectation lower when 0 is in the support of Ψ. Thus, the only price that would make the designer indifferent is zero. $\qquad\square$

This claim implies that the protocol designer aims for maximum block utilization, highlighting a point of conflict with miners, who may have different objectives, such as profit maximization.

Example 4. *(Technological Block Size Targets) Suppose that the designer has a target block size, denoted by q^{target}, that she aims to achieve. She might also allow some degree of deviation from the target block size, which we can represent as $S(q) = \ell\{q - q^{target}\}$, where ℓ stands for some loss function. For instance, a square loss function could be used to penalize deviations from the target:*

$$S(q) = -\left(q - q^{target}\right)^2 \tag{5}$$

17

Claim 5. *Under a technological block size target, the protocol designer prefers quantity controls over price controls. In particular, for the square loss function, the expected block size under optimal price controls $\mathbb{E}[q]$ is less than the target q^{target}, and the loss is given by*

$$\mathbb{E}[(q(\Psi) - q^{target})^2] = \frac{Var(\Psi)}{\mathbb{E}[\Psi^2]}(q^{target})^2 \tag{6}$$

Proof. Refer to Appendix C.2. □

This loss quantifies the variance in the block size, relative to the target, that arises because of the fluctuations in demand Ψ when the price is optimally chosen ex ante. This highlights that the loss for the protocol designer is larger when the demand shifter has high variance.

3.2.2 Validators' Monopoly Power

Given a price p per unit of block space and a fixed block reward R, the protocol profits are[4]

$$\Pi = R + \mathbb{E}\left[pq - C(q; \eta)\right]. \tag{7}$$

Assuming that users and application developers optimize resource usage, the cost to the validator becomes

$$C(q; p_x, \eta) = \min_{x \in \mathbb{R}_+^N} c(x_1, \dots, x_N; \eta) \tag{8}$$

subject to (2). The bundle x can be interpreted as the various resources that constitute a user transaction, such as bandwidth and computational operations. Let us consider

---

[4]Here, I abstract from the fact that not all fees collected go to the validators and so the profits of a monopolist validator could differ from the protocol profits.

that c is homogeneous of degree 1 in x.[5] We then have

$$C(q; p_x, \eta) = \Gamma(\eta, p_x) q \qquad (10)$$

The expression for the marginal cost Γ is derived in Appendix C.3.

A monopolist validator would then maximize profits in equation (7). In contrast to the protocol designer, who systematically prefers to set quantities ex ante, the monopolist validator might prefer either the price-setting or the quantity-setting regime, depending on the degree of demand uncertainty.

3.3   Bargaining Problem

I model the resolution of the potential conflict between the protocol designer and the validator by assuming that the price- or quantity-setting regime is determined by Nash bargaining over the protocol profits. The protocol designer and validators commit ex ante to a fixed base fee (price-setting) or fixed block space (quantity-setting) before uncertainty is realized. In practice, such a process is implemented by a set of rules in the TFM of the blockchain to which validators and blockchain designers agree. Even though the validator has ultimate control over which transactions, of what size and at what price can be included in a block, sophisticated mechanisms can be encoded to enforce prices and quantities. Protocol revenue can be diverted in part to the protocol treasury, burned, or rebated to users for the purposes of implementing the TFM; this design feature is beyond the scope of this paper.[6] The objective therefore balances social welfare and technological considerations while ensuring that validators have enough profit to be willing to provide their validator services.

---

[5]A typical example is the Cobb–Douglas cost function

$$c(x_1, \ldots, x_N; \eta) = \eta \prod_{i=1}^{N} x_i^{\varepsilon_i} \quad \text{such that} \quad \sum_{i=1}^{N} \varepsilon_i = 1 \qquad (9)$$

[6]See Roughgarden (2021).

The following objective captures this Nash bargaining game:

$$\mathcal{V} = \mathbb{E}\left[S(q)\right]^{1-\beta} \mathbb{E}\left[pq - C(q;\eta)\right]^{\beta} \tag{11}$$

In this objective, the parameter $\beta \in [0;1]$ captures validators' bargaining power. $\beta = 1$ means that the outcome maximizes validator profits, while $\beta = 0$ means that the outcome optimizes for the protocol designer's objective captured by the function $S(q)$.

Price Controls: Assuming that the block space demand follows the isoelastic demand curve derived in (3), with a price elasticity of demand $\varepsilon > 1$, and that the block size limit is not binding, the equilibrium block size lies on the demand curve, i.e., $q = \Psi \left(\frac{p}{p_m}\right)^{-\varepsilon}$. The problem of setting optimal prices then becomes

$$\mathcal{V}^p = \max_{p \in \mathbb{R}_+} \mathbb{E}\left[S\left(\Psi \left(\frac{p}{p_m}\right)^{-\varepsilon}\right)\right]^{1-\beta} \left[(p - \Gamma) \times \Psi \left(\frac{p}{p_m}\right)^{-\varepsilon}\right]^{\beta} \tag{12}$$

Quantity Controls: If the block size is set at q, the transaction is included in the block at the price that clears markets ex post: $p = p_m \left(\frac{q}{\Psi}\right)^{-\frac{1}{\varepsilon}}$. Then, the value of setting the optimal block space is

$$\mathcal{V}^q = \max_{q \in \mathbb{R}_+} \mathbb{E}\left[S(q)\right]^{1-\beta} \left[\left(p_m \left(\frac{q}{\Psi}\right)^{-\frac{1}{\varepsilon}} - \Gamma\right) \times q\right]^{\beta} \tag{13}$$

The log-difference between the values of price controls and block space controls can be defined as follows:

$$\Delta^{\log} = \log \mathcal{V}^p - \log \mathcal{V}^q \tag{14}$$

To derive some insight into the choice between price and quantity controls, consider a blockchain designer's objective that accounts for social welfare with utility $S(q) = u(q) = q^{\nu}$ for $\nu > 0$. The following proposition establishes the relationship between the relative value of price controls, the price elasticity of demand, and other moments of

20

the shock to demand and marginal costs given and an arbitrary bargaining power β for validators.

Proposition 6. *Assume that (Ψ, η) follows a joint log-normal distribution. Then, for any $\beta > 0$, the relative value of price controls over quantity controls is given by:*

$$\Delta^{\log} = \frac{1}{2}\left(\left(\hat{\nu} - \frac{\bar{\nu}}{\varepsilon}\right)\sigma_\Psi^2 - 2(\varepsilon\nu - \beta)\sigma_{\Psi,\Gamma}\right) \tag{15}$$

where $\bar{\nu} = (1-\beta)\nu + \beta$ and $\hat{\nu} = (1-\beta)\nu^2 + \beta$.

Proof. Refer to Appendix C.3. ☐

We can interpret this equation first by looking at the limit for $\beta \to 1, \nu \to 1$, which gives

$$\Delta^{\log} = \frac{1}{2}(\varepsilon - 1)\left(\frac{1}{\varepsilon}\sigma_\Psi^2 - 2\sigma_{\Psi,\Gamma}\right)$$

In this case, price-setting is preferable to quantity-setting when (i) demand volatility is high and (ii) the covariance between demand and real marginal costs is low. Uncertainty in demand favors price controls, as block size adjustments can flexibly respond to demand fluctuations. Additionally, a positive correlation between marginal costs and demand disfavors price controls, as this would lead to the production of larger blocks when marginal costs are high. The price elasticity of demand, which dictates how quickly prices react to changes, mediates the degree to which the firm values (i) and (ii). A larger price elasticity of demand favors price controls. In general, these comparative statistics indicate that price-setting has an advantage as long as demand is relatively elastic, i.e., $\varepsilon > \bar{\nu}/\hat{\nu}$, and validators have enough bargaining power, $\beta > \varepsilon\nu$.

Taking Stock: The above result helps us understand the differences in the policies that determine fees and block space in Bitcoin and Ethereum. We can see that both blockchains are instances where price elasticity of demand is high $\varepsilon > 1$ and demand uncertainty is significant $\sigma_\Psi^2 \gg 0$.

The background provided in Section 2.1 suggests that Ethereum can be viewed

through the lens of this model as an instance where the bargaining power of validators is high $\beta \to 1$ (or is considered high by the protocol designers). In addition, since the proof-of-stake upgrade, the marginal cost for Ethereum validators has been virtually constant, so that $\sigma_{\Psi,\Gamma} \approx 0$. Proposition 6 states that, in this case, price-setting is the most favorable policy. This explains the adoption of the EIP-1559 price-setting policy for the Ethereum blockchain. Furthermore, Figure 1 shows that EIP-1559 has performed better since Ethereum's proof-of-stake upgrade, consistent with the correlation between validators' marginal costs and demand relative to miners' being lower in a proof-of-work protocol.

Bitcoin is distinguished as the first blockchain with an anonymous founder, and its core developers strongly emphasize decentralization and censorship resistance. As discussed in Section 2.1, most proposals to change Bitcoin's fees and block size policies have failed. Bitcoin can therefore be viewed through the lens of our model as an instance where the bargaining power of validators (here miners) is low $\beta \to 0$ (or is not attributed enough importance by protocol designers, given the low block space utilization rate still observed). In addition, it is safe to assume that under the proof-of-work protocol, miners' marginal cost is largely positively correlated with demand $\sigma_{\Psi,\Gamma} \gg 0$. Proposition 6 states that, in this case, price-setting is less effective.

In general, the key determinants of the advantage of price-setting in blockchains are the validators' bargaining power, the elasticity of demand, the validators' uncertainty about demand, and marginal costs. This insight will guide us in Section 4 in studying the implications of my results for Ethereum transaction fees.

3.4 Effect of Cryptocurrency Price Fluctuations

Cryptocurrency prices can be volatile, while users value transaction processing services in dollar or real terms. This section examines the impact of cryptocurrency price volatility on the choice between price and quantity controls. Let P denote the exchange rate between 1 USD and the cryptocurrency (equivalently, the inverse of the cryptocurrency price expressed in dollars). Another way to interpret P is as the exchange rate between

22

1 unit of consumption goods and the cryptocurrency. This real model accommodates variations in both the cryptocurrency price and the value of fiat currency. Users pay transaction fees in the cryptocurrency at a nominal price p, implying that the dollar (equiv. real) value of these payments is $\frac{p}{P}$. Meanwhile, Γ represents the dollar (equiv. real) marginal cost.

The following proposition, formulated for simplicity with $\beta = 1$ (though similar insights apply for other parameters), provides an equivalent to Proposition 6 in this context:

Proposition 7. *Suppose (Ψ, η, P) is jointly log-normal distributed. Then, the relative value of price adjustments over quantity adjustments is*

$$\Delta^{\log} = \frac{1}{2}(\varepsilon - 1)\left(\frac{1}{\varepsilon}\sigma_\Psi^2 - 2\sigma_{\Psi,\Gamma} - \varepsilon\sigma_P^2 - 2\varepsilon\sigma_{P,\Gamma}\right) \tag{16}$$

In addition to the findings of Proposition 6, the variance of the cryptocurrency price and the covariance between the cryptocurrency price and the dollar (equiv. real) marginal cost both decrease the relative advantage of price controls over quantity controls.

4 Implications for Ethereum Transaction Fees

In this section, I explore how my results can inform the design of Ethereum fee policies. Proposition 6 implies that, under the conditions of (15), any fixed block size target q^{target} can be improved upon by setting prices ex ante and letting quantities adjust. As discussed in Section 2, Ethereum's fee policies follow such an approach to guarantee blocks of average size q^{target}. How can prices be set iteratively and heuristically? Below, I define a family of simple TFMs that include EIP-1559, Ethereum's TFM. I study their dynamics, determine the shape and adjustment rate of the optimal mechanism within this family, and provide bounds on the target block size that align with the incentives of a monopolistic validator.

Definition 8. *(ADT-TFM) A TFM is called adaptive to a deterministic target (ADT) if there exists a deterministic block size, q^{target} (the target), and a deterministic function, f (the adjustment function), such that the base fee satisfies*

$$\frac{p_{t+1}}{p_t} = g\left(\frac{q_t - q^{target}}{q^{target}}\right) \tag{17}$$

Example 9. *(EIP-1559) The base fee in EIP-1559 is ADT with linear adjustment function $g(x) = 1 + d \times x$ where the adjustment parameter is $d = \frac{1}{8}$.*

Let q^* denote the optimal quantity control or the block size that a blockchain designer aims to achieve for a specific technological target, $S(q) = \delta\{q - q^{target}\}$. In this case, $q^* = q^{target}$. We consider a general demand curve, with price elasticity of demand $\varepsilon(q^{target})$ that is assumed to be fixed and uncertainty in demand represented by λ. In this context, a TFM is considered robustly optimal if, following a sudden change or shock in demand, it manages to bring the realized quantity as close as possible to the targeted level in the worst-case scenario. The following proposition determines the shape and slope of the optimal ADT-TFM.

Proposition 10. *Suppose that the demand curve is log-convex; the robustly optimal ADT-TFM is an exponential function with an adjustment parameter equal to the inverse price elasticity of demand, $d = \frac{1}{\varepsilon(q^{target})}$. In other words, $g(x) = \exp(d \cdot x)$ and*

$$p_{t+1} = p_t \exp\left(\frac{1}{\varepsilon(q^{target})} \frac{q_t - q^{target}}{q^{target}}\right) \tag{18}$$

The intuition of the proof in Appendix C.4 goes as follows. Let f denote the adjustment function of the optimal TFM and $p(q_t)$ the price that matches demand at block size q_t. The base fees then satisfy

$$\ln p_{t+1} - \ln p_t = \ln g \left(\underbrace{\frac{q_t - q^{target}}{q^{target}} \frac{p(q^{target})}{p(q_t) - p(q^{target})}}_{g(q_t)} \frac{p(q_t) - p(q^{target})}{p(q^{target})} \right) \tag{19}$$

24

Near q^{target}, we have:

$$g(q_t) \xrightarrow[q^{target}]{} \frac{q'(p(q^{target}))p(q^{target})}{q^{target}} = \varepsilon(q^{target}) \tag{20}$$

And if p_{t+1} maintains the block size near q^{target}, then

$$\ln p_{t+1} - \ln p_t \sim \frac{p(q_t) - p(q^{target})}{p(q^{target})} \tag{21}$$

Let x denote this price growth. From (19), we obtain $x = \ln \left(g \left(\varepsilon(q^{target}) \cdot x \right) \right) + o(x)$ for all x in the neighborhood of zero.

Solving this functional equality yields $g(x) = \exp \left(\frac{x}{\varepsilon(q^{target})} \right)$ in the neighborhood of zero. The proof extends this argument with uncertainty in demand and shows that this function is optimal for the worst-case demand scenario in demand fluctuations.

In particular, when the elasticity of demand is constant, expression (20) becomes an equality everywhere. The adjustment parameter is a constant and equals the inverse of the price elasticity of demand. Moreover, the adjustment function takes the form of an exponential function everywhere. Similarly, if we restrict the adjustment function to be linear or of the form $(1+d)^{\frac{q_t - q^{target}}{q^{target}}}$ as studied by Leonardos et al. (2022), the adjustment rate remains the inverse of the price elasticity of demand. This elasticity, however, captures the price elasticity of inclusion of a transaction in the next block. Given the user interface shown in Figure 2, users are less likely to change their price in a short period of time, so this elasticity will be larger than the price elasticity of inclusion of a transaction within 5–10 minutes, for which users can substitute waiting in the mempool.

Adjustment Parameter for Ethereum: I now approximate Ethereum's adjustment rate through the lens of my analysis. I use Ethereum data because of its widespread availability, the simplicity of its ADT-TFM, and the global usage of its blockchain.

A random sample of 100,000 blocks, encompassing 16,881,386 transactions, was

extracted from the complete set of Ethereum blocks. This sample spans from the introduction of EIP-1559 at the London hard fork (block number 12965000, August 5, 2021) to block number 17731768 (July 20, 2023). Additional random block subsamples from before and after the Ethereum merge (block number 15537393, September 15, 2022) are also analyzed.[7]

The median block in the sample contains 143 transactions. Each block is associated with a number and a timestamp, the total gas used by all transactions in the block (equivalent to q in the model), and an array of transactions. Each transaction includes information on its gas unit, gas price, and other metadata. I do not have random variation in supply to trace the demand curve here. Instead, informed by Lemma 1, I calculate the Pareto tail of transaction gas prices, as the nearest proxy for user valuations, for blocks of size around q^{target} to obtain the price $\varepsilon(q^{target})$. This approach has limitations that I discuss in Appendix D.

My favorite number is a Pareto coefficient of 12.62 for blocks of size within $\pm 5\%$ of the block size target (over 7252 blocks and 12965717 transactions), which yields an optimal adjustment rate of 7.92%. This is significantly below Ethereum's current adjustment rate of 12.5%. This result aligns with the finding of Leonardos et al. (2022), who simulate the dynamic system of EIP-1559 and find stability around the target block size only for adjustment parameters below 8%. Several alternative choices in Appendix D yield a range between 6.14% and 11% for the Ethereum optimal adjustment rate. My contribution clarifies that the adjustment rate encapsulates the economic concept of inverse price elasticity of demand, which must be measured or approximated on-chain.

Target Block Size and MEV: Now, let us determine the block size target that aligns with the optimal target of a monopolistic validator. The goal of such a block size target is to make the blockchain immune to a simple form of MEV—that is, to prevent the validator from including her own value-extracting transactions while simultaneously reducing the effective supply available to users. The following definition makes this

---

[7]The results are consistent when I sample 100,000 blocks from before and after the merge separately.

notion explicit.

Definition 11. *(Myopic-Miner Incentive Compatibility) A quantity target is myopic-miner incentive-compatible (MMIC) if a myopic miner, by creating no fake transactions and adhering to the suggested block size target q^{target}, maximizes her profit.*

The MMIC definition implies that a miner who aims to maximize her revenue should be motivated to comply with the proposed quantity target when choosing her block size ex ante.

Proposition 12. *Given any isoelastic demand curve, the target block size aligning with the monopolist validator's optimal target block size is expressed as*

$$\frac{q^{target}}{q^{\max}} = \left(\frac{\varepsilon}{\varepsilon - 1}\right)^{-\varepsilon} \mathbb{E}\left[\lambda^{\frac{1}{\varepsilon}}\right]^{\varepsilon} \tag{22}$$

Proof. Refer to Appendix C.5. □

This proposition states that the maximum block size should have an adequate buffer above the block size; otherwise, if the block size target is too high relative to the maximum block size, the monopolist validator will have incentives to fill the block up to the target size with her own value-extracting transactions. In particular, if $q^{\max}$ is adjusted to coincide with user demand under average demand conditions, then $\frac{q^{\max}}{q^{target}} > e$. For the price elasticity found above, I obtain that the ratio of the maximum block size to the block size target should be greater than 2.83 for Ethereum, while it is currently set at 2.

5 Conclusion

In this paper, I have studied different blockchain fee policies to allocate block space efficiently when there are various sources of uncertainty. Namely, I have compared the quantity-setting regime used by Bitcoin and the price-setting regime used by Ethereum under different sources of uncertainty. Price controls are optimal in an environment

with low validator bargaining power, high price elasticity of demand, high demand uncertainty, and high marginal costs during the validation process. In addition, a high variance of the cryptocurrency price mitigates the advantages of price controls. These insights help explain the difference between Bitcoin's and Ethereum's fee policies. Next, I have applied these insights to a family of fee policies to which the method used by Ethereum belongs. Under mild assumptions on the shape of the demand for block space, I find that a crucial parameter of the mechanism, the rate of adjustment of prices, equals the inverse price elasticity of demand for inclusion in the next block. Some calculations using Ethereum transaction data suggest that the rate at which Ethereum's fees are changed is faster than optimal.

Henceforth, understanding the economics of multidimensional fees is crucial, as transactions use various types of resources. The question of designing fee policies for durable resources is growing in importance as blockchain states expand significantly over time, particularly due to resources such as storage. Additionally, as some blockchain states may experience less congestion than others, it is imperative to explore fee policies that differentiate pricing based on varying demand levels rather than solely pricing block space. These are topics of ongoing and future research.

References

Akbarpour, Mohammad and Shengwu Li, "Credible auctions: A trilemma," *Econometrica*, 2020, *88* (2), 425–467.

Bahrani, Maryam, Pranav Garimidi, and Tim Roughgarden, "Transaction Fee Mechanism Design with Active Block Producers," *arXiv preprint arXiv:2307.01686*, 2023.

Buterin, Vitalik, "Blockchain resource pricing," *URL: https://ethresear. ch/uploads/default/original X*, 2018, *2*.

_ **et al.**, "Ethereum white paper," *GitHub repository*, 2013, *1*, 22–23.

Catalini, Christian and Joshua S. Gans, "Some Simple Economics of the Blockchain," *Commun. ACM*, jun 2020, *63* (7), 80–90.

Chung, Hao and Elaine Shi, "Foundations of transaction fee mechanism design," in "Proceedings of the 2023 Annual ACM-SIAM Symposium on Discrete Algorithms (SODA)" SIAM 2023, pp. 3856–3899.

Daian, Philip, Steven Goldfeder, Tyler Kell, Yunqi Li, Xueyuan Zhao, Iddo Bentov, Lorenz Breidenbach, and Ari Juels, "Flash boys 2.0: Frontrunning in decentralized exchanges, miner extractable value, and consensus instability," in "2020 IEEE Symposium on Security and Privacy (SP)" IEEE 2020, pp. 910–927.

Easley, David, Maureen O'Hara, and Soumya Basu, "From mining to markets: The evolution of bitcoin transaction fees," *Journal of Financial Economics*, 2019, *134* (1), 91–109.

Ferreira, Matheus VX, Daniel J Moroz, David C Parkes, and Mitchell Stern, "Dynamic posted-price mechanisms for the blockchain transaction-fee market," in "Proceedings of the 3rd ACM Conference on Advances in Financial Technologies" 2021, pp. 86–99.

Flynn, Joel P, George Nikolakoudis, and Karthik A Sastry, "A Theory of Supply Function Choice and Aggregate Supply," 2023.

Hinzen, Franz J, Kose John, and Fahad Saleh, "Bitcoin's limited adoption problem," *Journal of Financial Economics*, 2022, *144* (2), 347–369.

Huberman, Gur, Jacob D Leshno, and Ciamac Moallemi, "Monopoly without a monopolist: An economic analysis of the bitcoin payment system," *The Review of Economic Studies*, 2021, *88* (6), 3011–3040.

Klemperer, Paul D and Margaret A Meyer, "Supply function equilibria in oligopoly under uncertainty," *Econometrica: Journal of the Econometric Society*, 1989, pp. 1243–1277.

Lavi, Ron, Or Sattath, and Aviv Zohar, "Redesigning Bitcoin's Fee Market," *ACM Trans. Econ. Comput.*, may 2022, *10* (1).

Lehar, Alfred and Christine A Parlour, "Miner collusion and the bitcoin protocol," *Available at SSRN 3559894*, 2020.

Leonardos, Stefanos, Barnabé Monnot, Daniël Reijsbergen, Efstratios Skoulakis, and Georgios Piliouras, "Dynamical analysis of the eip-1559 ethereum fee market," in "Proceedings of the 3rd ACM Conference on Advances in Financial Technologies" 2021, pp. 114–126.

_ , **Daniël Reijsbergen, Daniël Reijsbergen, Barnabé Monnot, and Georgios Piliouras**, "Optimality Despite Chaos in Fee Markets," *arXiv preprint arXiv:2212.07175*, 2022.

Malik, Nikhil, Manmohan Aseri, Param Vir Singh, and Kannan Srinivasan, "Why bitcoin will fail to scale?," *Management Science*, 2022, *68* (10), 7323–7349.

Nakamoto, Satoshi, "Bitcoin: A peer-to-peer electronic cash system," *Decentralized business review*, 2008.

Ndiaye, Abdoulaye, "Blockchain Price vs. Quantities," *Available at SSRN*, 2024.

Nisan, Noam, "Serial Monopoly on Blockchains," 2023.

Reis, Ricardo, "Inattentive producers," *The Review of Economic Studies*, 2006, *73* (3), 793–821.

Roughgarden, Tim, "Transaction fee mechanism design for the Ethereum blockchain: An economic analysis of EIP-1559," *arXiv preprint arXiv:2012.00854*, 2020.

— , "Transaction fee mechanism design," *ACM SIGecom Exchanges*, 2021, *19* (1), 52–55.

Weitzman, Martin L, "Prices vs. Quantities," *The Review of Economic Studies*, 1974, *41* (4), 477–491.

Appendix

A   History of Block Size Changes in Ethereum

| Dates	Changes in Gas Limit	Reasons and Context
March 4th, 2016	3,141,592 to 4,712,388	Max gas increased by 1.5x, and minimum gas price reduced from 50 to 20 gwei (a denomination of the Ethereum cryptocurrency) to improve affordability and throughput.
September 22nd, 2016	4,712,388 to 1,000,000	Network experienced a DDoS attack, leading to a drastic reduction in block size for security measures.
September 22nd, 2016	1,000,000 to 1,500,000	DDoS attack was partially mitigated, allowing a limited increase in block size.
October 15th, 2016	1,500,000 to 500,000	Block size was decreased as a precautionary step before implementation of a hard fork to address security vulnerabilities.
October 19th, 2016	500,000 to 3,000,000	Hard fork successfully implemented, security issues resolved, leading to a substantial increase in block size.
October 20th, 2016	3,000,000 to 1,500,000	Another DDoS attack occurred, prompting a reduction in block size to safeguard the network.
October 23rd, 2016	1,500,000 to 2,000,000	Successful mitigation of attacks led to increased block size, signaling return to stability.
November 24th, 2016	2,000,000 to 3,300,000	Continued stability and growing user base justified another increase in block size.

|		
December 5th, 2016	3,300,000 to 4,000,000	Network achieved consistent stability, allowing a further increase in block size.
June 3rd, 2017	4,000,000 to 4,712,388	Increase in network activity and user engagement necessitated a rise in block size.
June 29th, 2017	4,712,388 to 6,283,184	New target gas limit set at 4,700,000 to better match growing ecosystem demands.
December 10th, 2017	6,283,184 to 8,000,000	Rise in transaction volume driven by Cryptokitties NFT required an increase in block size.
September 19th, 2019	8,000,000 to 10,000,000	Tether's migration to the Ethereum blockchain led to increased transaction demands, prompting a block size increase.
June 19th, 2020	10,000,000 to 12,000,000	Miner consensus to increase block size was reached, supporting the growing Ethereum ecosystem.
July 25th, 2020	12,000,000 to 12,500,000	Minor increase following another round of miner agreements, aimed at fine-tuning network performance.
April 21st, 2021	12,500,000 to 15,000,000	Berlin hard fork led to efficiency improvements, enabling a substantial increase in block size.
August 5th, 2021	15,000,000 to 30,000,000	London hard fork brought about major improvements in transaction fee predictability and network efficiency, justifying a block size doubling.

Table A1: Table of history

B Capacity Utilization

B.1 Demand Factors

For my analysis, I identified the number of active addresses, token prices, and transaction fees as potential determinants of block space demand. For Bitcoin (BTC) only, I
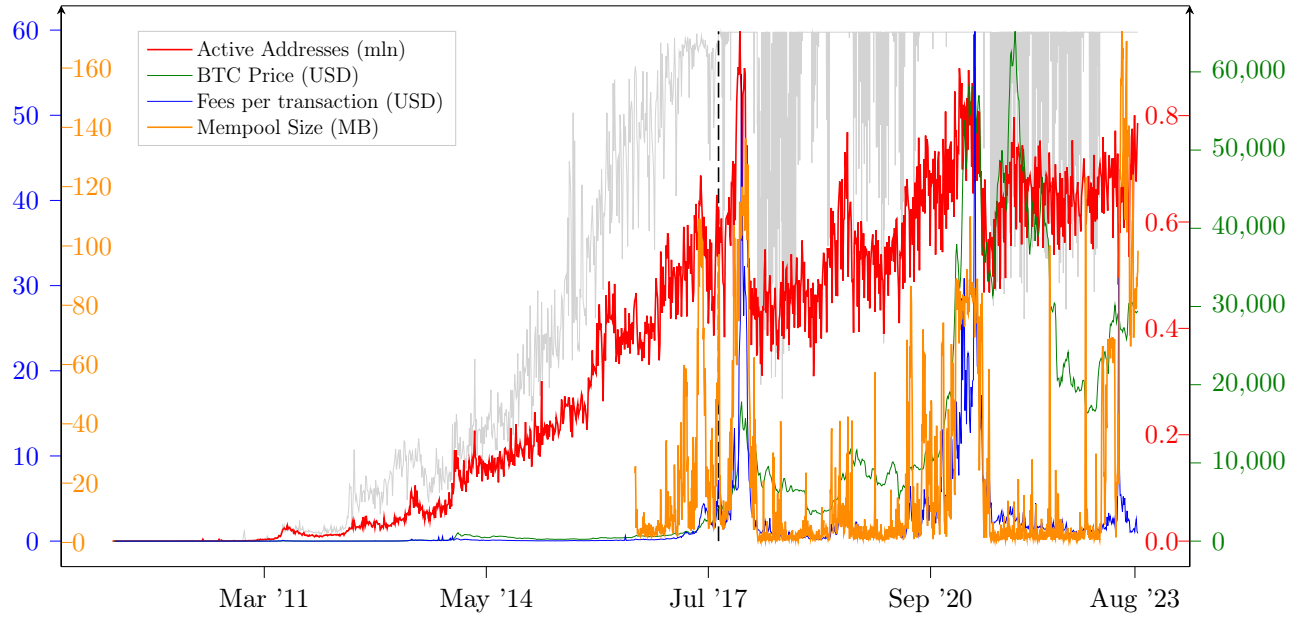
(a) Bitcoin network demand factors per day against utilization rate
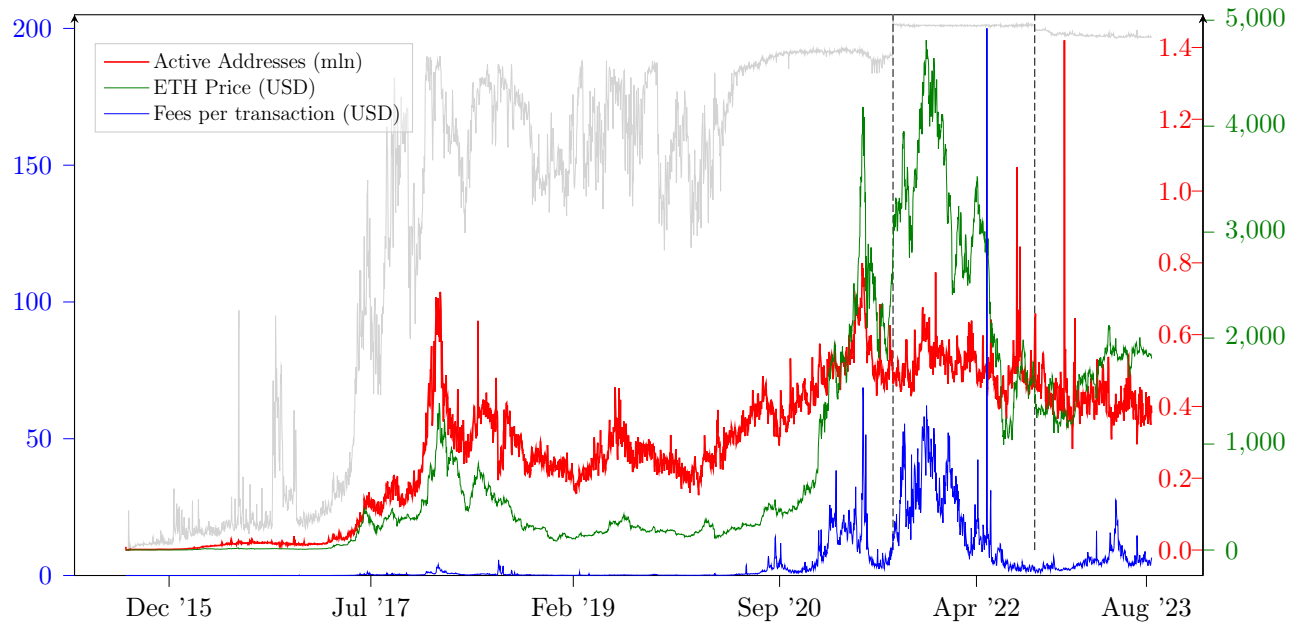
(b) Ethereum network demand factors per day against utilization rate

Figure A1: Time series of Bitcoin and Ethereum demand factors

also added the size of the mempool, i.e., the pool of transactions yet to be confirmed and included in a block.

For BTC, the top graph of Figure A1 shows that the number of active addresses has a strong correlation with the block utilization rate, as it acts as a good proxy for demand. Similarly, transaction fees show a tight link with the utilization rate, capturing the fact that users must offer a higher fee to be picked by miners in periods of block congestion. As explained in Lehar and Parlour (2020), mempool size is not a perfect predictor of block utilization, as miners can leave blocks empty, even when there are transactions waiting, to extract more profits. Finally, the BTC price has a loose relationship with the utilization rate, possibly because of its high volatility due to speculation.

For Ethereum (ETH), the bottom graph of Figure A1 shows that, before the London fork, the number of active addresses once again had the highest correlation with block utilization rates, best representing users' demand for transactions. Both transaction fees and the ETH price have stronger correlations with block fullness than their BTC counterparts. After the implementation of EIP-1559, gas levels stabilized consistently at the target level, suggesting that the implementation of the new fee system successfully achieved its objective. As a consequence, the block utilization rate became uncorrelated with its previously valid demand-side determinants.
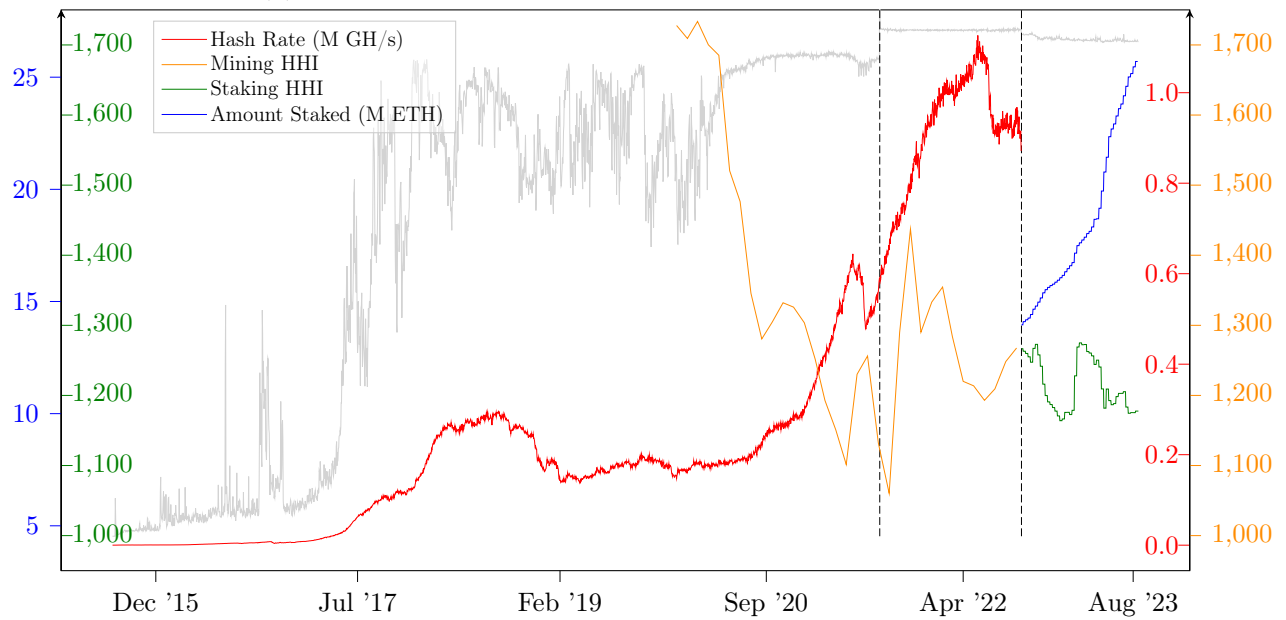
B.2 Supply Factors

For my analysis, I identified the computing power of miners and the concentration rate of mining pools as potential determinants of block space supply. For ETH only, I considered the total amount of ETH staked and the concentration of validator pools after the proof-of-stake update.

For BTC, the top graph of Figure A1 shows that the amount of computing power invested into mining does not affect the block utilization rate. I measure it using the hash rate, which measures how many guesses are made per second to solve the code to mine the next block. Regarding mining pool concentration, computed as the Herfindahl–Hirschman index (the sum of the squares of individual market shares) from
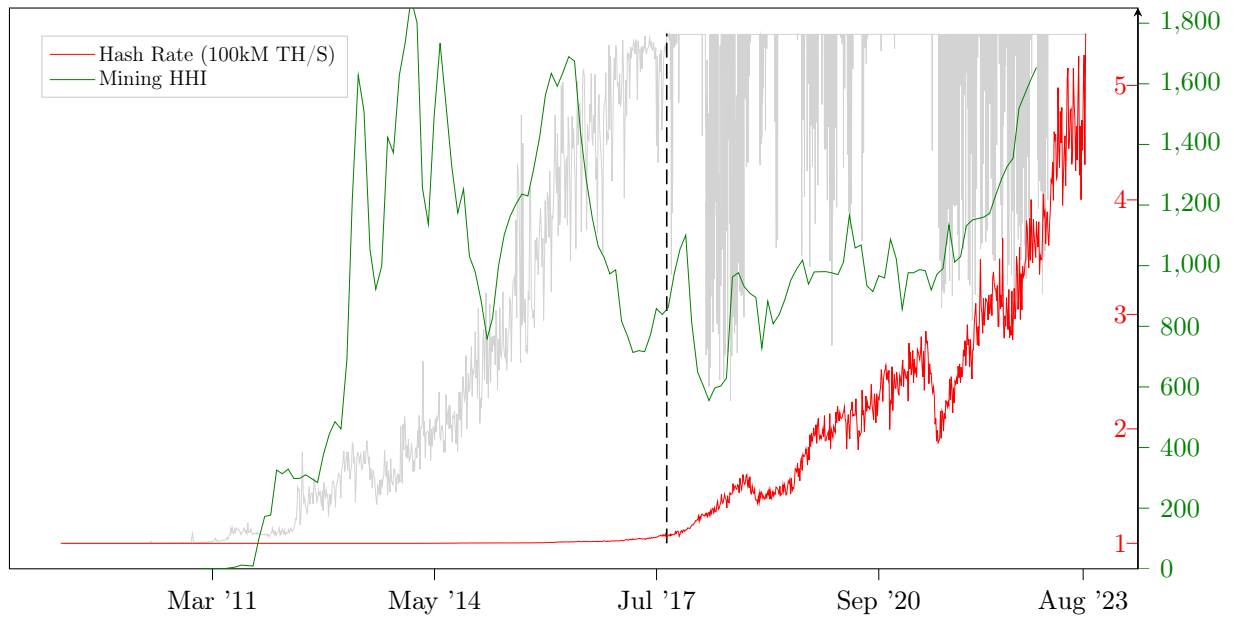
(a) Bitcoin network supply factors against utilization rate

(b) Ethereum network supply factors against utilization rate

Figure A1: Time series of Bitcoin and Ethereum supply factors

the shares of blocks mined in a one-month period, the graph seems to support the hypothesis that miners exercise their market power by leaving blocks less than full, as periods of higher HHI are usually accompanied by utilization rates below 100%.

For ETH, the bottom graph of Figure A1 shows that, under both proof of work and proof of stake, the computing power (or the amount of ETH staked, of which 32 ETH are required to activate a validator software), does not affect the utilization rate, similarly to what we observe for BTC. In contrast to the BTC case, however, the pool concentration does not affect the block utilization rate either. The HHI measures (from the share of blocks mined in a one-month period under proof of work and from the share of ETH staked over a one-month period under proof of stake) are not correlated with the utilization rate, which is particularly noticeable after the stabilization of the utilization rate post–London fork.

C   Analytic Proofs

C.1   Proof of Lemma 1

At a price p, demand for block space is the measure of users' willing to pay p for transaction inclusion, i.e., $\lambda q^{\max} \bar{F}(p)$. This yields the demand curve $p = \left(\bar{F}\right)^{-1}\left(\frac{q}{\lambda q^{\max}}\right)$. The price elasticity of demand is defined by (negative) the percentage change in quantity demanded over the percentage change in price, i.e., $-\frac{dq/q}{dp/p}$. Since from the demand curve $q = \lambda q^{\max} \bar{F}(p)$ and $dq/dp = -\lambda q^{\max} f(p)$, the demand elasticity is $\frac{pf(p)}{1-F(p)}$.

When F is a Pareto distribution with scale p_m and shape α,

$$\bar{F}(p) = Pr(v > p) = \begin{cases} \left(\frac{p_m}{p}\right)^{\alpha} & \text{for } p \geq p_m \\ 1 & \text{for } p < p_m \end{cases} \tag{23}$$

so that, above the minimum price p_m, demand is

$$q = \lambda q^{\max}\left(\frac{p_m}{p}\right)^{\alpha}$$

Therefore, we obtain

$$\frac{p}{p_m} = \left(\frac{q}{\lambda q^{\max}}\right)^{-\frac{1}{\alpha}}$$

C.2 Proof of Claim 5

The optimal ex ante quantity choice is just $q = q^{target}$ for which the loss is zero. The optimal ex ante price choice solves

$$\min_{p \in \mathbb{R}^+} E\left[\left(\Psi \cdot \left(\frac{p}{p_m}\right)^{-\varepsilon} - q^{target}\right)^2\right] \tag{24}$$

Denote $x \equiv \left(\frac{p}{p_m}\right)^{-\varepsilon}$. The first-order condition for the choice of p (resp. x) in (24) is

$$x = \frac{\mathbb{E}[\Psi] q^{target}}{\mathbb{E}[\Psi^2]} \tag{25}$$

The expected block size is then

$$\mathbb{E}[\Psi x] = \frac{\mathbb{E}[\Psi]^2 q^{target}}{\mathbb{E}[\Psi^2]} \leq q^{target} \tag{26}$$

Replacing (25) in the value of the loss function (24) yields

$$\frac{\mathbb{E}[\Psi^2] - \mathbb{E}[\Psi]^2}{\mathbb{E}[\Psi^2]} (q^{target})^2 = \frac{\text{Var}(\Psi)}{\mathbb{E}[\Psi^2]} (q^{target})^2$$

C.3 Proof of Proposition 6

We first find the expression of the marginal cost Γ in (10). The first-order condition is

$$c_i(x_1, \ldots, x_N; \eta) = \gamma p_{x_i} \tag{27}$$

where γ is the Lagrangian of constraint (2). Since c is homogeneous of degree 1, we have

$$c(x_1, \ldots, x_N; \eta) = \sum_{i=1}^{N} c_i(x_1, \ldots, x_N; \eta) x_i = \gamma \sum_{i=1}^{N} p_{x_i} x_i = \gamma q \tag{28}$$

Therefore, $\Gamma = \gamma$. Evaluating at $q = 1$ yields

$$\Gamma(\eta, p_x) = c(x_1(1, p_x, \eta), \ldots, x_N(1, p_x, \eta); \eta) \tag{29}$$

To prove the proposition, we now take logarithms of the blockchain designer's objective and maximize over p and q. The first-order conditions for the price choice and quantity choice are

$$\frac{\varepsilon(1-\beta)\nu}{p^*} + \frac{\varepsilon\beta}{p^*} = \frac{\beta \mathbb{E}[\Psi]}{p^* \mathbb{E}[\Psi] - \mathbb{E}[\Gamma\Psi]} \tag{30}$$

$$\frac{(1-\beta)\nu}{q^*} + \frac{\beta}{q^*} = \frac{\beta/\varepsilon p_m(q^*)^{-1-1/\varepsilon} \mathbb{E}[\Psi^{1/\varepsilon}]}{p_m(q^*)^{-1/\varepsilon} \mathbb{E}[\Psi^{1/\varepsilon}] - \mathbb{E}[\Gamma]} \tag{31}$$

Denote $\bar{\nu} = (1-\beta)\nu + \beta$. Then, we obtain

$$p^* = \frac{\varepsilon\bar{\nu}}{\varepsilon\bar{\nu} - \beta} \frac{\mathbb{E}[\Gamma\Psi]}{\mathbb{E}[\Psi]} \tag{32}$$

$$q^* = \left(\frac{\varepsilon\bar{\nu}}{\varepsilon\bar{\nu} - \beta} \frac{1}{p_m} \frac{\mathbb{E}[\Gamma]}{\mathbb{E}[\Psi^{1/\varepsilon}]} \right)^{-\varepsilon} \tag{33}$$

The log values of price controls and quantity controls are then

$$\log \mathcal{V}^p = -\varepsilon\bar{\nu} \log(p^*/p_m) + (1-\beta)\log(\mathbb{E}[\Psi^\nu]) + \beta \log(p^* \mathbb{E}[\Psi] - \mathbb{E}[\Psi\Gamma]) \tag{34}$$

$$\log \mathcal{V}^q = \bar{\nu} \log(q^*) + \beta \log(p_m(q^*)^{-1/\varepsilon} \mathbb{E}[\Psi^{1/\varepsilon}] - \mathbb{E}[\Gamma]) \tag{35}$$

Replacing the optimal choices with their values in (32) and (33), we obtain

$$\log \mathcal{V}^p \;=\; -\bar{\nu}\log(p^*/p_m) + (1-\beta)\log(\mathbb{E}[\Psi^{\nu}]) + \beta\log(\frac{\beta}{\varepsilon\bar{\nu}-\beta}\mathbb{E}[\Psi\Gamma]) \qquad (36)$$

$$\log \mathcal{V}^q \;=\; \bar{\nu}\log(q^*) + \beta\log(\frac{\beta}{\varepsilon\bar{\nu}-\beta}\mathbb{E}[\Gamma]) \qquad (37)$$

Simplifying yields

$$\log \mathcal{V}^p - \log \mathcal{V}^q \;=\; \bar{\nu}\varepsilon\log\mathbb{E}[\Psi] \qquad (38)$$

$$+(\bar{\nu}\varepsilon - \beta)(\log\mathbb{E}[\Gamma] - \log\mathbb{E}[\Psi\Gamma])$$

$$-\varepsilon\bar{\nu}\log\mathbb{E}[\Psi^{1/\varepsilon}] + (1-\beta)\log\mathbb{E}[\Psi^{\nu}]$$

For the joint log-(Ψ, Γ), with mean

$$\mu = \begin{pmatrix} \mu_\Psi \\ \mu_\Gamma \end{pmatrix}$$

and variance–covariance matrix

$$\Sigma = \begin{pmatrix} \sigma_\Psi^2 & \sigma_{\Psi,\Gamma} \\ \sigma_{\Psi,\Gamma} & \sigma_\Gamma^2 \end{pmatrix}$$

we have

$$\log\mathbb{E}[\Psi] \;=\; \mu_\Psi + \frac{1}{2}\sigma_\Psi^2 \qquad (39)$$

$$\log\mathbb{E}[\Gamma] - \log\mathbb{E}[\Psi\Gamma] \;=\; -\mu_\Psi - \frac{1}{2}\sigma_\Psi^2 - \sigma_{\Psi,\Gamma} \qquad (40)$$

$$\log\mathbb{E}[\Psi^{1/\varepsilon}] \;=\; \frac{1}{\varepsilon}\mu_\Psi + (\frac{1}{\varepsilon^2})\frac{1}{2}\sigma_\Psi^2 \qquad (41)$$

$$\log\mathbb{E}[\Psi^{\nu}] \;=\; \nu(\mu_\Psi + \frac{1}{2}\nu\sigma_\Psi^2) \qquad (42)$$

Putting them together, we obtain the result

$$\log \mathcal{V}^p - \log \mathcal{V}^q = \frac{1}{2}\left(\left(\hat{\nu} - \frac{\bar{\nu}}{\varepsilon}\right)\sigma_\Psi^2 - 2(\varepsilon\nu - \beta)\sigma_{\Psi,\Gamma}\right) \qquad (43)$$

where $\hat{\nu} = (1 - \beta)\nu^2 + \beta$.

C.4 Proof of Proposition 10

Let us start by defining the notion of optimality in this dynamic context. Let q^t be the equilibrium quantity at time t. Denote as $x_t = \frac{q_t - q^{target}}{q^{target}}$ the percentage deviation from the target at time t. Denote as λ the arrival rate in normal times (i.e., the expected arrival rate). Consider a shock to the demand curve $\lambda_t^{-1} \equiv \lambda^{-1} + z_t$. At the protocol set price p_t, the quantity lies on the demand curve $q_t = \lambda_t q^{max} \bar{F}(p_t)$. The deviation from target x_t can be due to the shock to demand z_t or to a protocol price p_t that is not properly set so that q_t deviates from the target.

We have the expression $p_t = \bar{F}^{-1}(\frac{q_t}{q^{max}\lambda_t})$. From the expression of the ADT-TFMs, we have

$$p_{t+1} = \bar{F}^{-1}\left(\frac{q^{target}(1 + x_t)}{q^{max}\lambda_t}\right)g(d \times x_t) \tag{44}$$

Without loss of generality at time $t + 1$, demand returns to normal so that $\lambda_{t+1} = \lambda$.

Known Intensity of Demand: Suppose for now that the realization of z_t, i.e., λ_t, is known; then, the deviation from the target quantity at time $t + 1$ is

$$x_{t+1} = \frac{\bar{F}\left(\bar{F}^{-1}(\frac{q^{target}(1+x_t)}{q^{max}\lambda_t})g(d \times x_t)\right)}{\bar{F}(p^{target})} - 1 \tag{45}$$

We can see that by setting

$$g(d \times x_t) = \frac{\bar{F}^{-1}(\frac{q^{target}}{q^{max}\lambda})}{\bar{F}^{-1}(\frac{q^{target}(1+x_t)}{q^{max}\lambda_t})} \tag{46}$$

we guarantee that the quantity at time $t + 1$ is at the target. The issue is that demand λ_t is uncertain, so we look at the function f that performs in the worst-case scenario.

Unknown Intensity of Demand: Because demand is uncertain, the adjustment function can depend on the gap from target x_t but not on λ_t. Thus, we need to evaluate the deviation that is closest for the worst-case value of z_t. We have

$$\ln \bar{F}^{-1}\left(\frac{q_{t+1}}{q^{target}}\right) = \ln \bar{F}^{-1}(\frac{q^{target}(1+x_t)}{q^{\max}\lambda_t}) - \ln \bar{F}^{-1}(\frac{q^{target}}{q^{\max}\lambda}) + \ln g(d \times x) \tag{47}$$

Suppose that $-\ln \bar{F}^{-1}$ is concave; then, for any x_t and $z_t = \lambda_t^{-1} - \lambda^{-1}$,

$$\ln \bar{F}^{-1}(\frac{q^{target}}{q^{\max}\lambda}) - \ln \bar{F}^{-1}(\frac{q^{target}(1+x_t)}{q^{\max}\lambda_t}) \geq \frac{1}{\varepsilon(q^{target})}(x_t + z_t) \tag{48}$$

From (47), we have that $\ln g(d \times x)$ is the closest approximation of $\ln \bar{F}^{-1}(\frac{q^{target}}{q^{\max}\lambda}) -$ $\ln \bar{F}^{-1}(\frac{q^{target}(1+x_t)}{q^{\max}\lambda_t})$ that is independent of z_t. Therefore, $f(d \times x) = x/\varepsilon(q^{target})$; i.e., $d = \varepsilon(q^{target})$ and $f = \exp$.

C.5 Proof of Proposition 12

From equation (33), the optimal quantity for a monopolistic miner is, for $\beta = 1$,

$$q^* = \left(\frac{\varepsilon}{\varepsilon - 1}\frac{1}{p_m}\frac{\mathbb{E}[\Gamma]}{\mathbb{E}[\Psi^{1/\varepsilon}]}\right)^{-\varepsilon} \tag{49}$$

With $\Psi = \lambda q^{\max}$. Now, suppose that the minimum user valuation is greater than the expected marginal cost $p_m > \mathbb{E}[\Gamma]$. Then, by including her own transactions up to the block size limit $q^{\max}$ and paying the base fee to herself, the validator obtains a positive value in expectation. Therefore, MMIC requires that $p_m \leq \mathbb{E}[\Gamma]$; thus,

$$q^* \leq q^{\max}\left(\frac{\varepsilon - 1}{\varepsilon}\right)^{\varepsilon}\mathbb{E}[\lambda^{1/\varepsilon}]^{\varepsilon} \tag{50}$$

By Jensen's inequality, $\mathbb{E}[\lambda^{1/\varepsilon}]^{\varepsilon} \leq \mathbb{E}[\lambda]$. Thus, the block size limit is set to match user demand in expectation; then, $\mathbb{E}[\lambda] = 1$, and thus,

$$\frac{q^*}{q^{\max}} \leq \left(\frac{\varepsilon - 1}{\varepsilon}\right)^{\varepsilon} \tag{51}$$

The right-hand side is an increasing function for $\varepsilon > 1$ with limit e^{-1}.

These bounds provide valuable insights for studies of TFMs involving monopolistic validators (Nisan, 2023; Lavi et al., 2022) and TFMs designed to prevent validators from monopolizing all surplus (Bahrani et al., 2023).

Figure A1 illustrates how the upper bound of the ratio q^*/q^{max} changes with ε. This upper bound approaches an asymptote of $e^{-1} \approx 37\%$, and it reaches 95% of this limit when $\varepsilon = 10.42$. Ethereum currently sets the target block size to half the block size limit. The correct interpretation of this result is that any ADT-TFM with a target block size exceeding 37% of the block size that meets user demand in an average demand scenario would not be invulnerable to a simple form of MEV. This is because MMIC necessitates that the validator has no incentive to include her own value-extracting transactions while simultaneously reducing the effective supply available to users.
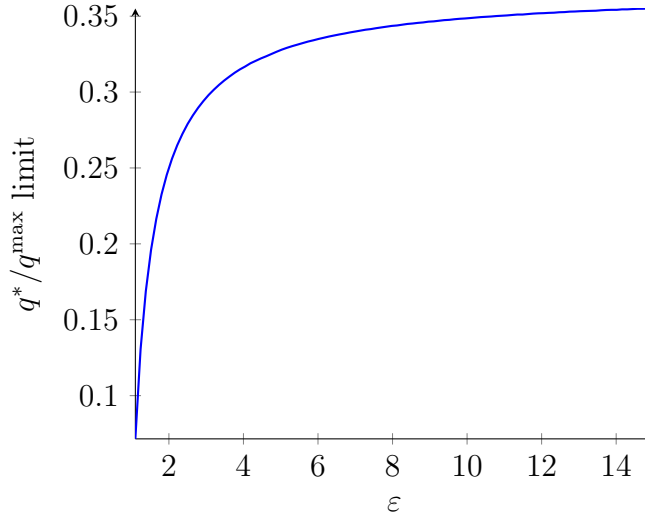

Figure A1: Optimal target block size for a monopolist validator as a function of ε

D   Numerical Examples

Methodology: The inference of a demand curve requires random variation in supply to distinguish between shifts along the demand curve and shifts in the demand curve itself. Nevertheless, such random variation in supply is rare

because of the programmatically defined rules of blockchains.

Instead, a different strategy, informed by the user demand model presented in Section 3, is adopted. Lemma 1 shows that, for any density f of user valuations, the price elasticity of demand is the tail ratio $\dfrac{pf(p)}{1 - F(p)}$. Specifically, if the distribution is Pareto, the price elasticity is its Pareto tail coefficient. Knowing the Pareto tail of the distribution of user valuations allows determination of the optimal adjustment parameter from Proposition 10 as the inverse of the Pareto tail coefficient.

In this analysis, transaction gas prices serve as the nearest proxy for user valuations, given the available data. A Pareto distribution is fitted to the empirical distribution of effective transaction gas prices in each randomly selected block to calculate the optimal adjustment rate. However, this approach is not without limitations.[8] First, gas prices censor user valuations at the lower end of the distribution because of the base fee. Second, pending transactions in the mempool, which carry lower base fees, are not included. Consequently, the estimate will reflect a heavier tail than the actual user valuation distribution. Therefore, the estimate of the Pareto tail coefficient is an underestimate, meaning its inverse—the optimal adjustment rate—will be overestimated. The adjustment parameters identified here should thus be considered an upper bound.[9] To address these limitations, several robustness exercises are performed, which include restricting the estimation to blocks with a minimum gas price below a certain threshold (to limit the censoring of low valuations) and to blocks that are less than full (to limit the censoring of mempool transactions). These robustness exercises do not alter the primary conclusions of this numerical analysis.

---

[8]As users demand different amounts of block space, each transaction is weighted by the gas units that it uses to fit the Pareto distribution.

[9]Given that the optimal adjustment rate found here is lower than its current value of 12.5%, this upper bound estimate offers valuable insights for the design of Ethereum's TFM.

Discussion: The estimate from a sample prior to the merge suggests an adjustment rate of 6.57% (tail coefficient 15.22), while the optimal adjustment rate for the blocks following the merge is 8.68% (tail coefficient 11.53). The observation that the current adjustment rate of 12.5% overshoots more before the merge than after aligns with the findings of Leonardos et al. (2022). The authors postulate that this discrepancy is because inter-block times were (approximately) exponentially distributed prior to the proof-of-stake upgrade whereas they are constant in Ethereum's proof-of-stake protocol. A constant block arrival rate more accurately reflects my model, suggesting that an estimate around 8% is more suitable for the current blockchain. One might wonder whose price elasticity our estimate represents and why it is so high (over 10). The adjustment rate represents the inverse elasticity of the marginal user submitting her transaction for inclusion in the next block. Given the low block size limit, which is set because of technological constraints, it is not implausible that a marginal decentralized finance (DeFi) user with sensitive transactions would exhibit significant demand elasticity, similarly to how high-frequency traders are sensitive to spreads.

Another consideration is that this analysis does not account for users whose transactions remain in the mempool for several blocks before confirmation. Notably, under EIP-1599, base fees do not decrease fast enough after a surge in demand. A TFM that responds to intra-day or intra-hourly demand variations would not need to adjust prices based on the size of the previous block. Instead, it could maintain fixed prices during high-demand periods, fill blocks, and monitor the mempool for price adjustments. However, mempool data are typically not recorded on-chain (i.e., as part of the immutable blockchain) and can be easily manipulated.

Alternative Calculations: This section presents the results of supplementary robustness checks to validate the primary numerical analysis findings. These checks are performed under various conditions to address potential concerns highlighted above, such as the base fee causing censoring of low valuations and the exclusion of pending mempool transactions. To investigate the consistency of the Pareto tail coefficient and the optimal adjustment rate, I adjust the selection of blocks within a size range of $q^{target}(1 \pm \delta\%)$ and different limits on base fees.

The estimations are performed on three samples: the full sample, the pre-merge sample, and the post-merge sample. Tables A2, A3, and A4 provide detailed results. The estimated optimal adjustment rates are consistently lower than the 12.5% adjustment rate and remain stable under various data partitionings. The estimate is smaller for the pre- than for the post-merge sample, as previously found. The adjustment rates decrease as the window around the target block size widens and the maximum base fee increases. Ethereum transaction fees are paid in units of gwei. The increase in rates as the max base fee limit becomes more restrictive (for blocks with a base fee of less than 30 gwei) can only produce thicker tails because of a restricted range and censoring. Variations based on δ, the window of the target block size, are quite robust, with an adjustment rate in the full sample estimation ranging from 7.33% to 8.03% for a more accommodating max base fee of 200 gwei. Estimates from the pre-merge and post-merge samples suggest that the optimal adjustment rate lies within the 6% to 10% window, where the latter serves as an upper limit.

Blockchain designers must adopt simple, robust, and principled methods for updating TFM parameters. However, updating parameters and the "rules of the game" as we go might not be best tack for fostering scalability. Considering nondeterministic adjustment rates for TFMs could provide a solution. Preliminary quantitative explorations using adjustment rates derived from prices and

| Parameters | | Outputs | | Observations |
δ	max base fee (gwei)	shape α	adjustment rate d	number of blocks
	200	12.45	8.03	7189
	100	11.83	8.45	6645
5%	60	11.01	9.08	5867
	30	9.50	10.53	4130
	200	12.77	7.83	43718
	100	12.09	8.27	40471
33%	60	11.26	8.88	35649
	30	9.48	10.55	25193
	200	13.64	7.33	78881
	100	12.62	7.92	70769
87.5%	60	11.53	8.67	60141
	30	9.50	10.53	41140

Table A2: Shape of Pareto fit α and optimal adjustment rate s for the different maximum gas prices (base fee) in units of gwei and selection of blocks within size $q^{target} \pm \delta\%$ (full sample estimation)

| Parameters | | Outputs | | Observations |
δ	max base fee (gwei)	shape α	adjustment rate d	number of blocks
	200	11.46	8.73	5088
	100	11.24	8.89	4962
5%	60	10.84	9.23	4688
	30	9.55	10.47	3547
	200	11.48	8.71	30029
	100	11.29	8.86	29454
33%	60	10.89	9.18	27884
	30	9.55	10.47	21288
	200	11.32	8.83	42042
	100	11.15	8.97	41348
87.5%	60	10.78	9.28	39426
	30	9.47	10.56	30890

Table A3: Shape of Pareto fit α and optimal adjustment rate s for the different maximum gas prices (base fee) in units of gwei and selection of blocks within size $q^{target} \pm \delta\%$ (post-merge sample estimation)

Parameters		Outputs		Observations
δ	max base fee (gwei)	shape α	adjustment rate d	number of blocks
	200	14.85	6.73	2101
5%	100	13.57	7.37	1683
	60	11.70	8.55	1179
	30	9.15	10.93	583
	200	15.59	6.41	13689
33%	100	14.22	7.03	11017
	60	12.57	7.96	7765
	30	9.09	11.01	3905
	200	16.29	6.14	36839
87.5%	100	14.69	6.81	29421
	60	12.96	7.71	20715
	30	9.58	10.44	10250

Table A4: Shape of Pareto fit α and optimal adjustment rate s for the different maximum gas prices (base fee) in units of gwei and selection of blocks within size $q^{target} \pm \delta\%$ (pre-merge sample estimation)

quantities of the preceding two blocks have shown promising results in terms of how well these rates reflect market conditions during the relevant periods. A more stable and manipulation-resistant approach could involve calculating an average elasticity over a range of prior blocks. Alternatively, introducing noise to the target block size, effectively the "supply curve", could help us infer demand fluctuations under normal conditions.